Hydrogel Bioadhesives with Extreme Acid-Tolerance for Gastric Perforation Repairing

Xingmei Chen,[a] Jun Zhang,[a] Guangda Chen,[a] Yu Xue,[a] Jiajun Zhang,[a] Xiangyu Liang,[a] Iek Man Lei,[a] Jingsen Lin,[a] Ben Bin Xu[b] and Ji Liu[a,c,d] ***

Hydrogel bioadhesives have emerged as one of the most promising alternatives to sutures and staples for wound sealing and repairing, owing to their unique advantages in biocompatibility, mechanical compliance and minimally invasive manipulation. However, only a few hydrogel bioadhesives have been successfully used for gastric perforation repairing, due to their undesirable swelling when in direct contacting with extremely acidic gastric fluids, thereby accompanying with a gradually-deteriorated adhesion performance. Herein, we develop an acid-tolerant hydrogels (ATGels) bioadhesive, which integrates two distinct components, an acid-tolerant hydrogel substrate and an adhesive polymer brush layer. The ATGels bioadhesive could form instant, atraumatic, fluid-tight and sutureless sealing of gastric perforation, and enable robust biointerfaces in direct contact with gastric fluids, addressing the key limitations with sutures and commercially-available tissue adhesives. Moreover, *in vivo* **investigation on gastric perforation of rat model validates the proposed acid-tolerant bioadhesion, and identifies the mechanisms for accelerated gastric perforation repairing through alleviated inflammation, which suppressed fibrosis and enhanced angiogenesis.**

Introduction

Gastric perforation, such as gastric ulceration and gastric cancer rupture, is one of the acutest abdominal diseases.[1] Severe gastric perforation can lead to peritonitis, septic shock, and even multiple organ disfunction syndromes, and so far surgical operation is the most reliable therapy in clinical settings.[2,3] Sutures made of biodegradable polymers (*i.e.* polyglycolic acid, polylactic acid, polylactic-*co*-glycolic acid or polyesterurethane) have been routinely used for repairing gastric perforation, however, they are associated with severe gastric tissue damage and inflammation of biological tissues caused by deep piercing and ischemia.[4–9] Besides, employing decellularized tissue matrix for sealing also carries a high risk of immune reactions, especially in the occasions with acute injuries or infections.[10] In light of these shortcomings, bioadhesive materials have become one of the most promising alternatives or adjuncts to sutures and staples for gastric wound sealing and repairing.[9,11,12]

In the past decades, the clinical needs have motivated tremendous efforts to develop bioadhesive materials that feature superior flexility, biocompatibility, robust tissue adhesion, excellent biodegradability and compatibility with the wet and dynamic biological environments.[9,11] Among these synthetic bioadhesives, hydrogel-based bioadhesives have emerged as one of the most promising approaches for sutureless wound sealing, particularly in emergency clinical settings, owing to their intrinsic similarity to tissues in the biological, mechanical, chemical and physical aspects.[9,11–14] Despite recent advancement in hydrogel-based adhesives for epidermal and/or *in vivo* wound sealing, such as DOPA-inspired hydrogels,[15,16] double-side tapes,[17–19] GelMA-based bioadhesive,[20,21] topological adhesion,[22] electrically-activated gelation,[23] dynamical host-guest hydrogels[24,25] and poly(*N*-acryloyl-2-glycine)-based hydrogel,[26] only a few hydrogel bioadhesives have been successfully applied for gastric repairing.[14,27–29] In cases of gastric perforations or defects with relatively small size, the tissue of the stomach can quickly update the gastric mucosa with the assistance of bioadhesives, thus spontaneously accelerating the gastric healing.[30,31] However, larger gastric perforations are routinely challenged by the leakage of gastric contents and peritonitis. Additionally, for radical gastrectomy with lymph node dissection, neoplasty is also accompanied with the repeated leakage due to the persistent tumor invasion.[32,33] In such clinical settings, during the long-term contact with extremely acidic fluids, the bioadhesives may experience undesirable swelling, and subsequent gradual deterioration in strength and interfacial robustness (**Fig. 1a-b**).[34] On the other hand, the dynamic motion of gastric tissues may also cause the interfacial fatigue failure, thus constituting a significant barrier against their uses as a minimally invasive technique.[13,35]

** [a] Department of Mechanical and Energy Engineering, Southern University of Science and Technology, Shenzhen, 518055, China.
E-mail: liuj9@sustech.edu.cn.
[b] Smart Materials and Surfaces Laboratory, Faculty of Engineering and Environment, Northumbria University, Newcastle upon Tyne, NE1 8ST UK.
[c] Shenzhen Key Laboratory of Biomimetic Robotics and Intelligent Systems, Department of Mechanical and Energy Engineering, Southern University of Science and Technology, Shenzhen, 518055, China.
[d] Guangdong Provincial Key Laboratory of Human-Augmentation and Rehabilitation Robotics in Universities, Southern University of Science and Technology, Shenzhen, 518055, China.

Supporting information for this article is available on the WWW under or from the author.

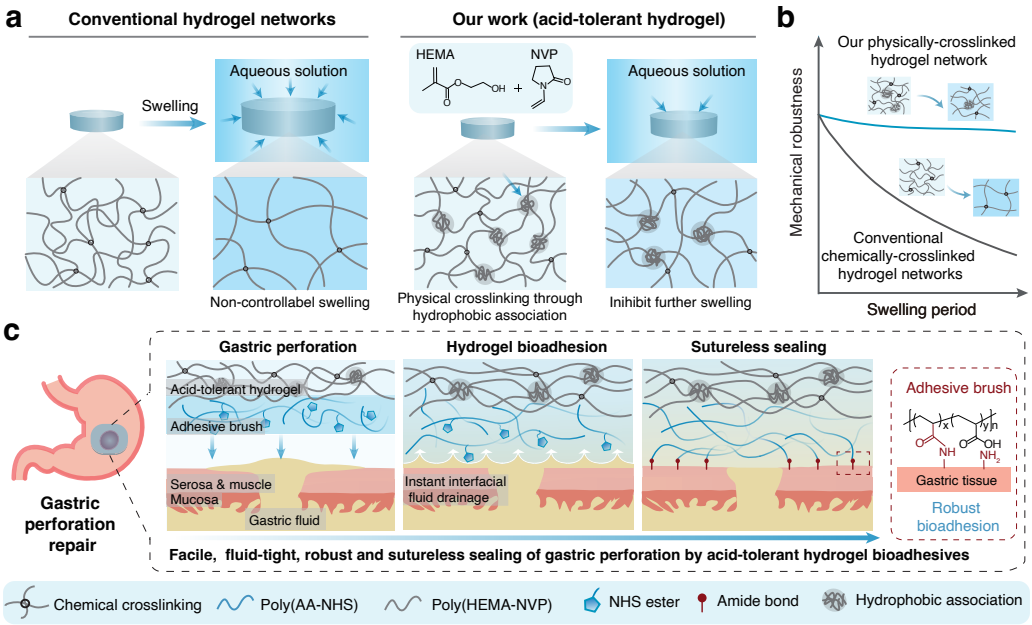

Figure 1. Design of our acid-tolerant hydrogel bioadhesives for gastric perforation sealing. a. Conventional chemically-crosslinked hydrogel networks swell drastically when soaked into water or fluids in extreme conditions (*i.e.* low pH). Our proposed hydrogel adhesives are physically-crosslinked through hydrophobic associations, of which the widely-distrubuted segregation substantially inhibits further swelling under such extreme conditions. **b.** Difference in the evolution of mechanical robustness of our proposed hydrogel networks, compared with conventional chemically-crosslinked hydrogel networks. **c.** Schematic illustration of our acid-tolerant hydrogel adhesives (ATGels bioadhesive) for gastric perforation sealing through the dry crosslinking mechanism, exploiting the interfacial water drainage and the covalent crosslinking between the NHS moieties (hydrogel part) and amine moieties (tissue part). The robust adhesion at the interface with gastric tissue is enabled by the distinct acid-tolerance of our hydrogel bioadhesives.

Herein, we report a new kind of synthetic hydrogel adhesives for sutureless repair of gastric perforation. Our hydrogel adhesive embodies three core functionalities that synergistically address the above-mentioned limitations. They are gastric fluid resistance, instant and tough adhesion to gastric tissues, and extraordinary long-term adhesion robustness under wet and dynamic *in vivo* conditions. To achieve these credentials, the hydrogel adhesives integrate two distinct components, an acid-tolerant hydrogel substrate (poly(2-hydroxyethyl methacrylate-*co*-*N*-vinypyrrolidone), poly(HEMA-NVP)) and an adhesive polymer brush layer (poly(acrylic acid-*co*-*N*-hydroxysuccinimide acrylate ester), poly(AA-NHS)). Such kind of hydrogel bioadhesives could form instant, atraumatic, fluid-tight and sutureless sealing of gastric perforation, and also robust adhesion interfaces in direct contact with gastric fluid (pH $\sim$ 2.0), addressing the key limitations existing in sutures and commercially-available tissue adhesives and sealants. We also investigate the possible mechanism underlying the accelerated repairing of gastric perforation aided by our ATGels bioadhesive through histopathology and immunofluorescence analyses in a rat model.

Results and Discussion

Instant, tough and robust bioadhesion under gastric conditions.

To validate this concept, we synthesize the acid-tolerant hydrogels from the copolymerization of hydroxyethyl methacrylate (HEMA), *N*-vinypyrrolidone (NVP) and PEGDA (2 kDa, crosslinker, **Supplementary Fig. S1**). Thanks to the well-established presence of phase segregation through hydrophobic association coupled with intrinsic van der Waals interactions and hydrogen bonds,[36,37] the as-obtained poly(HEMA-NVP) hydrogel reaches its equilibrium state after 8-h soaking in a simulated gastric fluid (SGF, mixture of 150 mM sodium chloride and 10 mM hydrochloric acid, pH 2.0), while maintaining its high water content (78 *wt.%*) and mechanical robustness (strength, modulus and toughness) in the following 240 h (**Supplementary Fig. S2-3**). To endow the poly(HEMA-NVP) hydrogel with an excellent tissue adhesion capability, we further graft adhesive polymer brushes (poly(AA-NHS)), which consist of acrylic acid (AA) and *N*-hydroxysuccinimide acrylate ester (AA-NHS), onto the poly(HEMA-NVP) hydrogel substrates (**Supplementary Fig. S1**). Hereafter, the as-obtained brush hydrogel bioadhesives are referred to as ATGels bioadhesives for abbreviation. It is deserved to mention that introduction of the a polymer brush layer slightly changes the mechanical properties of the ATGels; moreover, the as-obtained ATGels samples exhibit a gastric tissue-level mechanical compliance (**Supplementary Fig. S4**). To achieve an instant and tough bioadhesion, our ATGels bioadhesives adopt the well-established dry crosslinking mechanism that exploit the synergetic contribution from non-covalent interactions (*i.e.* hydrogen bonding and electrostatic interactions) and covalent bonds between the NHS (adhesive side) and amine moieties (tissue side, **Fig. 1c**).[17–19] Upon further hy-

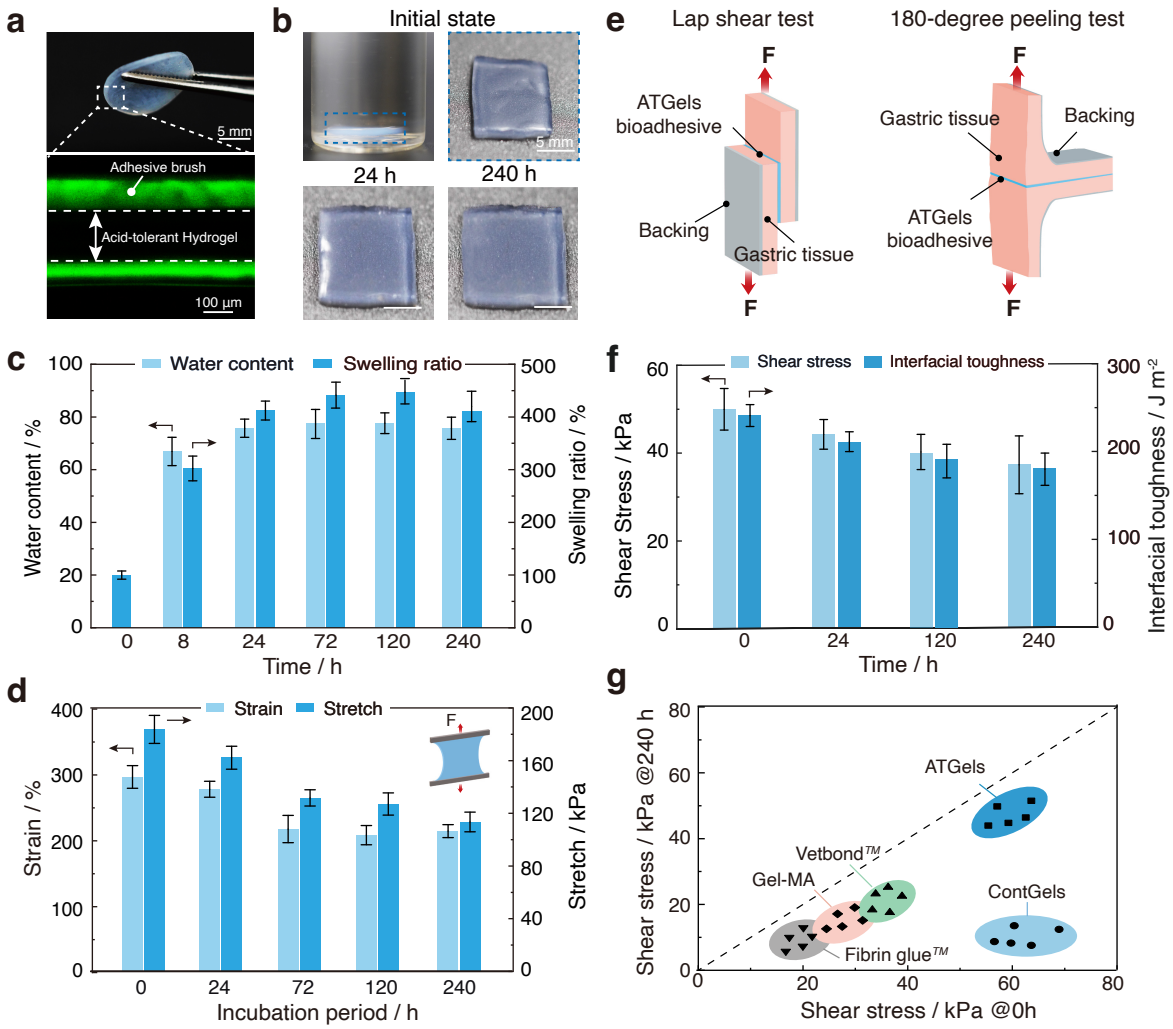

Figure 2. Mechanical performance and acid-tolerance of our hydrogel bioadhesives. a. Representative image of an ATGels sample (top) and fluorescence image showing its distinct three-layered structure (bottom). Note: the polymer brushes are labeled with FITC. **b.** Image of the ATGels samples before and after soaking in SGF for 24 h and 240 h. **c.** Evolution of the water content and the swelling ratio of the ATGels samples during soaking in SGF medium (pH 2.0) in 240 h, and the data at 0 h refers to hydrogel film at its dry state. **d.** Summary of strain and stretch of the ATGels samples after soaking in the SGF medium (pH 2.0) for different periods of time, and the data at 0 h refers to the hydrogel samples at its initial wet state. **e.** Schematic illustration of the lap shear and the 180-degree peeling tests used here for quantifying the interfacial shear strength and toughenss, respectively. **f.** Adhesion stability of the adhered joints between the porcine gastric tissues and the ATGels bioadhesive in SGF medium (pH 2.0) for 240 h. **g.** Comparison chart summarizing the adhered joints between the various bioadhesives before and after incubating within the SGF medium (pH 2.0) for 240 h. The data in **c**, **d** and **f** were presented as the mean ± S.D. ($n = 5$).

dration and adhesion on wet tissues, the ATGels dry films turn into hydrogel networks with desirable mechanical compliance with the gastric tissues. Moreover, due to the protonation of poly(acrylic acid) moieties in gastric fluids (pH of 1.0 ∼ 3.0), swelling of the polymer brush layer is efficiently inhibited.[28] Therefore, issues associated with non-controllable hydrogel swelling and mechanical deterioration during the repairing of gastric perforation could be effectively mitigated (**Fig. 1c**).

Confocal laser scanning microscopic (CLSM, **Fig. 2a**) and scanning electron microscopic (SEM, **Supplementary Fig. S5**) images manifest the unique three-layer structure as depicted in (**Fig. 1c**), with a brush layer of 50 μm and a hydrogel substrate of 500 μm in the wet state. As known to us, most hydrogels are susceptible to structural, compositional and mechanical deterioration in extremely acidic environments, *i.e.* gastric fluids.[13,34,35] Here, the water content of our ATGels reach a plateau within 24 h in SGF (pH 2.0) at body temperature (37 °C), afterwards, no change in the water content, swelling ratio and the overall mass is detected (**Fig. 2c**). Moreover, our ATGels demonstrate high strength over 100 kPa and toughness over 200 J m^{-2} (**Fig. 2d** and **Supplementary Fig. S6**) even after 240-h soaking within the SGF medium.

To evaluate the bioadhesive performance of our ATGels, we then conduct lap-shear and 180° peeling tests on joints of porcine gastric tissues adhered with our bioadhesive (**Fig. 2e**). The tests confirm the high interfacial toughness of the ATGels bioadhesive (*ca.* 300 J m^{-2}) and its robust bioadhesion with an interfacial toughness of 200

J m^{-2} after 240 h soaking in the SGF medium (**Supplementary Fig. S7-8**). Moreover, such interfacial toughness surpasses those commercially-available cyanoacrylate-based (*i.e.* Vetbond^{TM}) and hydrogel-based tissue sealants (*i.e.* Fibrin glue^{TM}, $<$ 50 J m^{-2}, **Supplementary Fig. S9**). Additionally, in order to avoid postsurgical adhesion and corresponding severe surgical complications during the *in vivo* gastric repairing,[26,38] outer-side surface modification of ATGels bioadhesives is conducted with bovine serum albumi (BSA), which could de-activate the adhesion capability of the outer-side surface. As shown in **Supplementary Fig. S10**, due to the reaction between the NHS ester of the ATGels bioadhesive and BSA, the adhesion experiences a 14-fold decrease in shear strength and a 9-fold decrease in interfacial toughness after soaking in BSA (1 *wt.%*) solution for 1 minute. Our ATGels bioadhesive is also applicable to other biological tissues with comparable interfacial toughness, *i.e.* porcine kidney, heart, spleen and liver (**Supplementary Fig. S11**). We further prepare PAA-NHS bulk hydrogels (also known as ContGels) following a previous report,[17] and use them as a control for comparison. In sharp contrast, due to the severe swelling ($>$ 10 $\times$) in the acidic SGF medium medium (**Supplementary Fig. S12**), the ContGels experience a fourfold decrease in strength and a eightfold decrease in toughness in 8 h (**Supplementary Fig. S13**), while the interfacial toughness decreases over 10 times in 24 h (**Supplementary Fig. S7c**), making it unsuitable for gastric defect repairing.

Fig. 2g compares the interfacial shear stress of commercially-available bioadhesives (*i.e.* Fibrin glue^{TM} and Vetbond^{TM}), ContGels bioadhesive, Gel-MA hydrogel, and our ATGels bioadhesives before and after 240 h soaking in SGF (pH 2.0). It is shown that the commercially-available bioadhesives exhibit relatively low shear stress ($<$ 30 kPa), and could not sustain the acidic environment. Remarkably, our ATGels bioadhesive exhibits a much higher shear stress (40$\sim$60 kPa) compared to the commercially-available bioadhesives (*i.e.*, Fibrin glue^{TM} and Vetbond^{TM}) and the tough hydrogel adhesives (*i.e.*, GelMA hydrogels and ContGels)[17,20,21] after 240-h soaking in SGF. In addition, the relatively low shear stress of the commercially-available bioadhesives ($<$ 30 kPa) significantly impair their ability to sustain the acidic environment. Overall, the slight change in the shear stress after long-term soaking in extremely acidic environments outperforms most hydrogel bioadhesives, offering promising applicability in repairing gastric perforation.

Ex vivo gastric perforation sealing

Ex vivo gastric perforation sealing is demonstrated on an explanted porcine stomach (from a local butcher's shop). An incision of *ca.* 5 cm is created with a scalpel, in order to simulate the gastric perforation (**Fig. 3a**). We then promptly seal the perforation with our ATGels bioadhesive, and transfer the sealed stomach into a PBS buffer solution, mimicking the biological fluidic environment (**Fig. 3b**). SGF medium (pH 2.0) is then filled into the stomach, while red food dye is used to stain the SGF for visual effect. No liquid leaking is observed for both the ATGels bioadhesive and the control group (ContGels bioadhesive), corroborating the instant and tough bioadhesion resulting from the dry-crosslinking mechanism.[17] The ContGels bioadhesive layer drastically swells within 4 hours, and a burst leak occurs within 8 hours, indicating the adhesion failure (**Supplementary Movie S1**). In contrast, our ATGels adhesion remains robust during the after 48-h of observation, indicating a fluid-tight sealing of the perforated stomach (**Supplementary Movie S2**). Due to the difficulties in storing porcine stomach samples under ambient condition, we did not extend our observation period, however, we expect that the robust sealing could last much longer, which will be evaluated in the following *in vivo* tests.

The microstructure and conformity of the adhesion interface between the ATGels bioadhesive and gastric tissue are further studied with SEM (**Fig. 3c**). Similar to the SEM images of the ATGels samples (**Supplementary Fig. S5**), a distinct three-layer structure is observed even after bonding with gastric tissues. Additionally, the magnified microstructure shows conformal adhesion interface between the ATGels bioadhesive and the gastric tissue, corroborating the robust interfacial adhesion. Since the hydrogel bioadhesive is applied as a dry polymer film, the resulting rapid hydration of the polymer films into hydrogel networks and the interfacial water drainage of the gastric tissues drive the penetration of polymer chains into the tissues. Thus, the robust and seamless interfacial adhesion is attributed to the synergy of the physical interlocking and the chemical bonding between the poly(AA-NHS) chains and the collagen fibers of the tissues.[11,20,39]

In addition to adhesion strength and toughness, burst pressure is another key character to evaluate the robustness of wound sealants for biological organs, since the adhesive layers have to withstand a certain pressure for maintaining the inner fluid and/or air flow. As shown in **Fig. 3d**, we build a setup to quantify the burst pressure, where a piece of gastric tissue is fixed onto the holder, and an air dispenser is used to gradually tune the pressure. A hole of 5 mm in diameter is created with a scalpel, and subsequently sealed with the ATGel bioadhesives. Upon 5 s of interfacial wet adhesion, air pressure is gradually increased to exert force on the sealed incision, and the critical pressure is taken as the burst pressure when the sealing failed (n = 5). The measured burst pressure reaches as high as 33.9 kPa (254 mmHg) for our ATGels bioadhesive (**Fig. 3d**), much higher than that of the commercially-available tissue sealants, such as Vetbond^{TM} and Fibrin glue^{TM}. Moreover, the burst pressure of ATGels bioadhesive is remarkably higher than the intra-gastric pressure (0.67$\sim$3.3 kPa or 5$\sim$25 mmHg).[40] This property is particularly beneficial for gastric sealants as the fluidic pressure exerted on gastric tissue can be occasionally high during digestion.

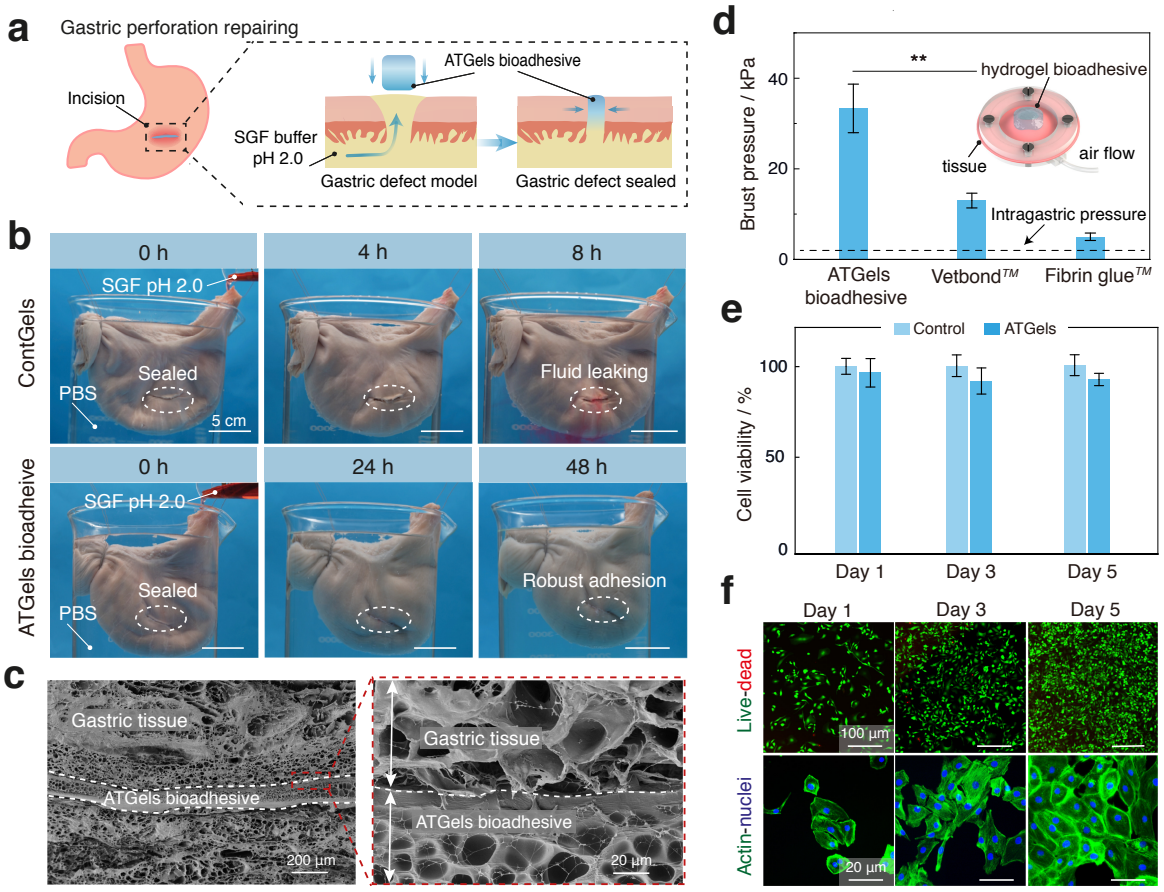

Figure 3. *Ex vivo* **demonstrations of of the robust sealing ability in gastric perforation and** *in vitro* **biocompatibility of the ATGels bioadhesives. a.** Schematic illustration of the ATGels bioadhesive for gastric perforation repairing. **b.** Photos of sealing the porcine stomach defects with the ATGels bioadhesive, where the porcine stomach is filled with SGF *ex vivo* prior to immersion in PBS to demonstrate the acid-tolerant bioadhesion. Control group is conducted with the PAA-NHS bulk hydrogels (ContGels) bioadhesive (scale bar: 5 cm). **c.** SEM of the adhesion interface between the ATGels bioadhesive and gastric tissues. Magnified image clearly shows the distinct three-layer structure of the ATGels bioadhesive, and also the conformal adhesion interface between the ATGels bioadhesive and the gastric tissue. **d.** Summary of the burst pressures of the ATGels bioadhesive and commercially-available tissue bioadhesives (Vetbond^{TM} and Fibrin glue^{TM}). **e.** Cell viability of GES-1 cells against ATGels bioadhesive after incubation for 1, 3 and 5 days. **f.** Representative images of GES-1 cells with live/dead staining (top, scale bar: 100 μm) after incubation on ATGels samples for different periods, as well as cell images with F-actin and DAPI nuclear staining (bottom, scale bar: 20 μm). The data in **d** and **e** are presented as the mean $\pm$ S.D. ($n = 5$). $^{**}p < 0.01$.

Biocompatibility and biodegradability of the hydrogel bioadhesives

The hydrogel bioadhesive for gastric perforation repairing must be biocompatible, permitting the cells at the injured areas to migrate and proliferate for further integration and repairing. We therefore co-culture the human gastric epithelial cells (GES-1) with our ATGels samples and NHS molecules to evaluate the *in vitro* biocompatibility and cell behaviours during culture. No obvious difference in quantitative cell viability (through CCK-8 assay) is observed between the ATGels, control groups (PBS) (**Fig. 3e**), as well as the NHS molecules (**Supplementary Fig. S14**) and corresponding byproducts during the cell culture, indicating the excellent biocompatibility of our ATGels bioadhesive. We observe a uniform monolayer of the GES-1 cells on the ATGels substrate, featuring normal cell morphologies. Additionally, nearly no dead cells (red luminance) are observed upon live/dead cell staining, and the GES-1 cells substantially proliferate over tenfold within 5 days (**Fig. 3f**). These results reveal the positive role of our ATGels in the migration and proliferation of GES-1 cells, thus promoting the gastric defect repairing.

The *in vitro* degradability of our ATGels bioadhesive is assessed through PBS incubation in the presence of esterase (**Supplementary Fig. S15**), while *in vivo* degradability is evaluated through subcutaneous implantation in a rat model for 56 days (**Supplementary Fig. S16**). Similar to the *in vitro* biodegradation behaviours (**Supplementary Fig. S15**), the size of the implanted ATGels samples gradually decreases (**Supplementary Fig. S16b-c**), accompanying with an increased pore size (**Supplementary Fig. S17**), and the remaining mass is below 10% after 56 days. To probe the physiological side-effects associated with the biodegradation byproducts, we conduct further histological analysis on tissues in close contact with the implanted hydrogel samples. No obvious inflammatory response is detected after Day 7 and Day 28, suggesting the absence of macrophages and su-

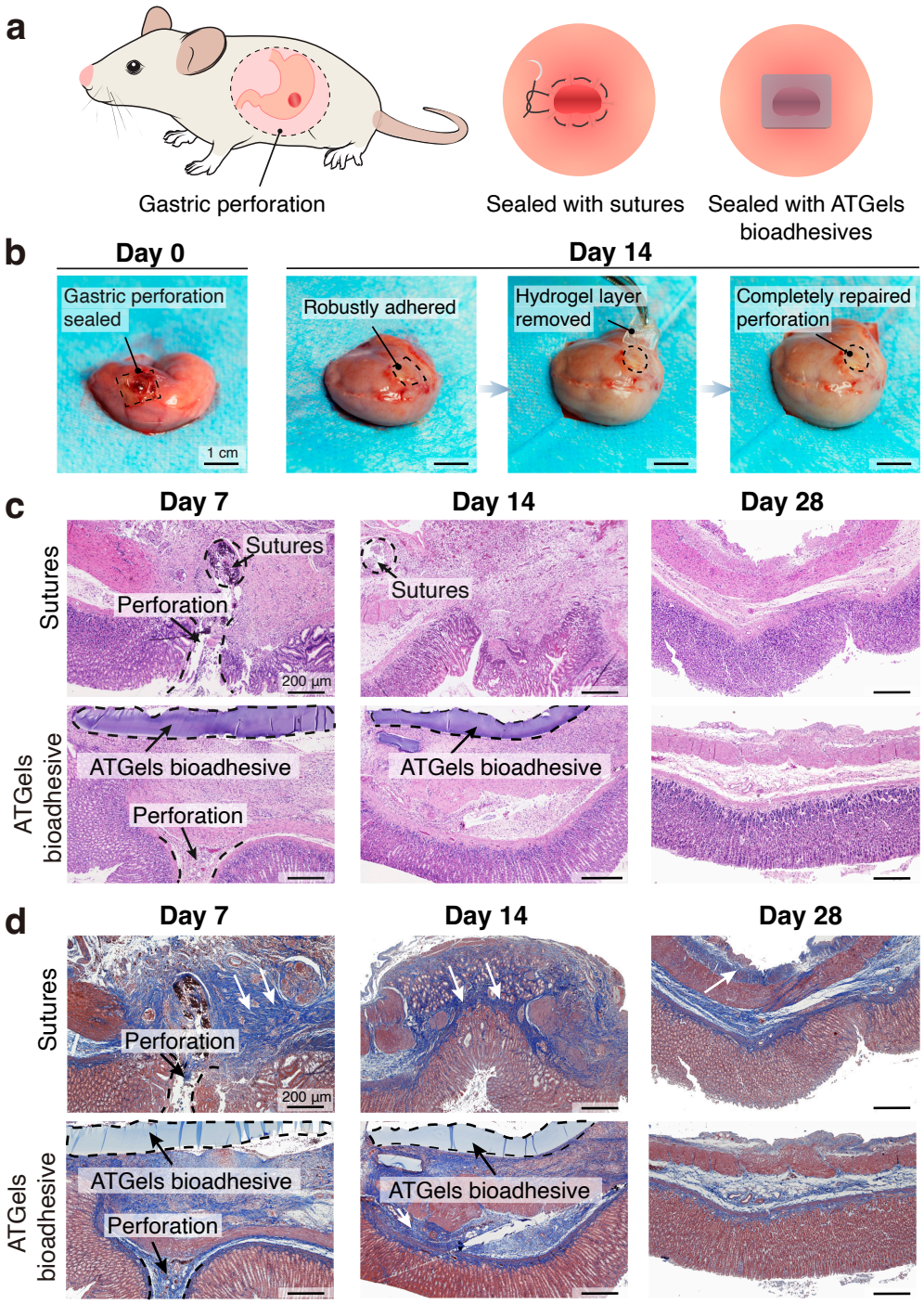

Figure 4. Sutureless repair of gastric perforation in rat models. a. Schematic illustration for the gastric perforation repairing with sutures or ATGels bioadhesive in rat stomachs. **b.** Images illustrating the use of the ATGels bioadhesive to seal gastric perforation on Day 0, and a repaired stomach after 14 days. The ATGels adhesive robustly adheres onto the stomach at Day 14, and completely sealed perforation is confirmed when the hydrogel bioadhesive is carefully removed (scale bar: 1 cm). **c-d.** Hematoxylin-eosin (**c**) and Masson staining (**d**) of gastric perforation repaired by sutures and the ATGels bioadhesives after 7, 14, and 28 days (scale bar: 200 μm). White arrows indicate the presence of collagen fibers. Note: For a specific sample at predesignated time interval, HE and Masson staining images were taken from two locations close to each other, except for the suture group on Day 14.

perior *in vivo* biocompatibility of the ATGels bioadhesive. Moreover, an accelerated degradation of the implanted hydrogel samples was observed after Day 7, and negligible fragmentation was observed after 56 days (**Supplementary Fig. S18a**). We further demonstrate that *in vivo* biodegradation of ATGels bioadhesive poses no damage to other organs (*i.e.* heart, liver, spleen, lung and kidney) by histological analysis through HE staining (**Supplementary Fig. S18b**).

In vivo gastric perforation repairing

Having demonstrated the unique acid-tolerance, *ex vivo* instant and tough adhesion with gastric tissues, long-term robustness and superior biocompatibility and biodegradability, we then evaluate the gastric perforation repairing using our ATGels bioadhesive. Perforation is created on a SD rat model (200∼300 g, n = 15, **Fig. 4a**) that is treated as severe gastric injury. The perforation is then sealed with our ATGels bioadhesive, while sealing with sutures is taken as a control. We find that the ATGels bioadhesive could form a robust adhesion with the gastric serosal tissue and seal a 5-mm perforation in rat stomach immediately within a few seconds (**Fig. 4b** and **Supplementary Movie S3**), similar to the *ex vivo* results (**Fig. 3**). In contrast, the point-wise wound closure by sutures takes much longer time ($>$ 2 min) to seal and can cause puncture-induced tissue damage (**Supplementary Movie S4**). Overall, the ATGels bioadhesives offer simple, consistent and fully conformal sealing. During a follow-up period of 14 days, the hydrogel bioadhesion remains robust. By carefully removing the hydrogel layer, no gastric fluid leakage occurs, suggesting the successful sealing of the gastric perforation (**Fig. 4b**). After 28 days, perforations in both ATGels bioadhesive and suture groups repair completely (**Supplementary Fig. S19**). It is notable that due to the BSA treatment, postsurgical adhesion and corresponding surgical complications are substantially suppressed, similar to previous reports.[26,38]

Further histological analyses through HE and Masson staining reveal that the gastric perforation is repaired by fibrous tissues, predominantly composed of collagenous networks and fibroblasts, while a denser fibrous tissue is resulted in the case where the perforation is treated with sutures (**Fig. 4c-d**). It is worth mentioning that the ATGels bioadhesive remains robustly adhered onto the defects and surrounding tissues, and tissue interstitial porosity and edema are observed after 14 days of sealing with the ATGels bioadhesive. Moreover, the typical three-layered structures of the gastric walls around the perforation are clearly observed after 28 days (**Fig. 4c-d**). In contrast, the mucosal layer is not completely closed at 14 days after sealing with sutures, meanwhile the local stress created by suture penetration causes drastic deformation of the local tissues and contraction of the overall stomach (**Fig. 4c-d**). Notably, other organs (*i.e.* heart, kidney, liver, spleen and lung) in both groups are in their normal states without signs of inflammation or damage caused by gastric fluids leaking (**Supplementary Fig. S20**) after 28 days of repairing with the ATGels bioadhesive. These above findings support our hypothesis that the ATGels bioadhesive is capable of sealing severe gastric perforation without the aid of additional staples or sutures in a preclinical animal model. Further experiments are warranted to evaluate the long-term fate of hydrogel sealants, as well as the therapeutic efficacy of our ATGels bioadhesives on even larger perforation of large animal models.

Further immunocytochemical analysis is conducted to evaluate the capability of our ATGels bioadhesives in gastric perforation healing. Although perforation healing is found on Day 7 when sutures are used, severe tissue inflammation at the defect areas (serosal and mussel layer) is clearly observed, as evidenced by the presence of a large amount of macrophases (CD68, 46%),[41] that is in sharp contrast to the group treated with the ATGels bioadhesive (26.1%, **Fig. 5a, e**). Excessive inflammation could stimulate the over-expression of collagen and subsequent fibrosis, leading to scars formation.[28,42] Masson staining in **Fig. 4d** also reveals that the collagen fibers are at a significantly higher level for the suture group, in sharp contrast to the ATGels bioadhesive.

Re-epithelization and angiogenesis are key factors contributing to gastric perforation repairing.[27,29] We then stain PCNA (proliferation marker) and CD31 (endothelial cell marker) for further analysis. Immunohistochemistry staining of PCNA, a proliferation marker of G1/S phase, displays significantly less proliferating cells (37 %) after the perforation is sealed with the ATGels bioadhesive for 14 days, while 54% for the suture group (**Fig. 5b, f**). Noteworthily, the expression ratio of PCNA decreases to 16.4% at 28 days sealing with the ATGels bioadhesive, indicating a complete repairing of the wound into normal tissues. On the other hand, the PCNA percentage remains as high as 30% in the suture group, suggesting that more time is needed for a complete perforation repairing. Similarly, after 14-day sealing, immunostaining of α-SMA (α-smooth actin and mature blood vessels) and CD31 (endothelial cell marker for new blood vessels) possesses significantly higher microvessel density in the ATGels bioadhesive group (**Fig. 5d, g, h**, **Supplementary Fig. S21**). All these immunohistochemical results reveal that the use of the ATGels bioadhesive as gastric perforating sealants could effectively accelerate the transition from inflammation to proliferation phase, suppressing excessive fibrosis to promote ECM remodelling, and providing nutrition for angiogenesis.[43] The gastric perforation repairing capability of our ATGels bioadhesives remarkably surpasses that of suture, offering promising prospect for clinical surgeries.

Conclusions

In this work, we have reported an acid-tolerant hydrogel (ATGels) bioadhesive by integrating an acid-resistant hydrogel substrate with an adhesive polymer brush layer. The ATGels bioadhesive is capable of achieving instant, tough, fluid-tight and sutureless sealing of gastric perforation, and enabling robust adhesion interfaces in direct contact with gastric fluids. Taking advantage of the full set of functionalities of our ATGels bioadhesive, we further demonstrate that the use of our ATGels bioadhesive as a sutureless sealant could accelerate the gastric perforation repairing in a rat model through alleviated inflammation, suppressed formation of fibrosis and increased angiogenesis. While the curernt work provides systematic studies on the

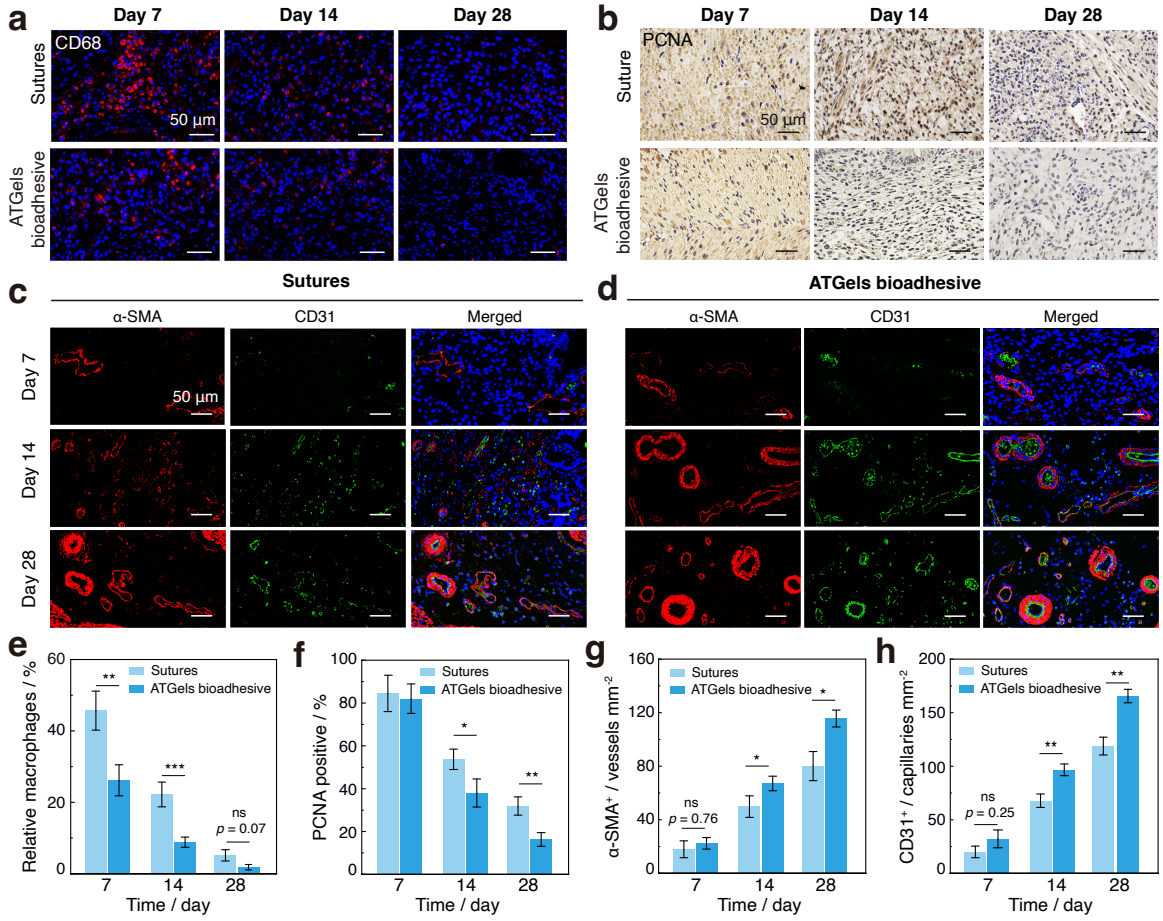

Figure 5. Immunocytochemistry analysis of the process of gastric perforation repairing by sutures and hydrogel bioadhesive treatment. a-d. Immunostaining for CD68 (red, **a**), PCNA (dark brown nuclei, **b**), α-smooth muscle actin (α-SMA, red) and CD31 (green, **c-d**) of gastric perforation repaired by suture and ATGels bioadhesive after 7, 14, and 28 days. **e-h.** Quantification of the relative percent of macrophages (CD68, **e**), PCNA-positive cells percent (**f**), α-SMA-positive small arteries (**g**), and CD31-positive capillaries (**h**) from the immunostaining images of the repaired gastric sections with suture and ATGels bioadhesive treatment. **g.** , and **h.** The scale bars in **a-d** are 50 μm, data in **e-h** are presented as the mean $\pm$ S.D. ($n = 5$). $^{*}p < 0.05$, $^{**}p < 0.01$, $^{***}p < 0.001$.

proof-of-concept efficacy of our ATGels bioadhesive for gastric perforation repairing, future investigation on larger animals (*e.g.* rodent and porcine models) with larger-size perforation (*i.e.* $>$ 10 mm)[32,33] is necessitated to further define the applicability and efficacy before testing in clinical settings. Additionally, our current ATGels bioadhesive enables an complete *in vivo* biodegradation within *ca.* 8-week after implantation, while tailored *in vivo* biodegradation kinetics through optimizing both the hydrogel substrates and polymer brushes could improve the repairing efficacy, by considering the healing dynamics of each medical case. Moreover, by integrating our ATGels bioadhesive with various delivery techniques, such as endoscopic stapler,[38] it may offer minimally-invasive treatment for gastric perforation repairing and gastrectomy repairing in diverse clinical settings.

Materials and Methods

Preparation of the acid-tolerant hydrogels (ATGels) bioadhesive.

The ATGels bioadhesive was prepared by grafting polymer brushes onto the of poly(HEMA-NVP) hydrogel substrates. First, a hydrogel precursor solution of HEMA (0.8 mol L^{-1}), NVP (1.2 mol L^{-1}), PEGDA (M_n = 2 kDa, 0.3 *wt.%*) and Irgacure 2959 (0.5 *wt.%*) was prepared. After degassing through centrifugation, the precursor solution was transferred into a glass mold and exposed to UV irradiation (365 nm, 20 mW cm^{-2}, 60 min). The as-obtained Poly(HEMA-NVP) hydrogels were dialyzed against excessive amount of Mill-Q water to remove the unreacted small-molecule residues, following by air-drying (thickness of 200 μm) and storing under -20 °C before use.

To graft the polymer brushes, the Poly(HEMA-NVP) film was first soaked into a benzophenone solution (10 *wt.%* in diethyl ether) for 2 min. After that, the Poly(HEMA-NVP) film was rinsed with diethyl ether and dried completely with nitrogen flow. Then, the Poly(HEMA-NVP) film was im-

mersed in an aqueous monomer solution containing 20 *wt.%* AA and 2 *wt.%* AAc-NHS monomer. After UV radiation (365 nm, 20 mW cm^{-2}) for 30 min, the as-obtained hydrogel samples were dried in air and then stored at -20 °C prior to further experiments.

Mechanical tests.

The stress-strain curves of the hydrogels were recorded with a tensile machine, at a constant deformation rate of 20 mm min^{-1}. All the hydrogel samples for tensile tests were cut into a dumbbell shape with a laser cutter, and treated with simulated gastric fluid (SGF, pH 2.0) medium for designated periods prior to tensile tests. Fracture toughness of the ATGels bioadhesive was quantified by employing the pure-shear test at a deformation rate of 50 mm min^{-1}.

Standard lap-shear and 180° peeling tests were performed on the adhered joints of between various tissues and our ATGels bioadhesive, while commercially-available bioadhesives, such as Vetbond^{TM} and Fibrin glue^{TM}, and PAA-NHS bulk hydrogels (ContGels) were also tested as controls. Biological tissues, such as porcine skin or gastric tissues, were cut into slices with a dimension of 50 mm (*L*) × 10 mm (*W*) × 0.5 mm (*t*), and then cleaned with PBS buffer. The adhered tissue joints were fabricated by laminating two tissue slices together with our dry hydrogel adhesive films, followed by slight pressing (*ca.* 1 kPa) for 10 seconds before mechanical tests. Nylon papers (*ca.* 100 μm in thickness) were adhered on the other side of the tissues as stiff backings using cyanoacrylate glue, in order to avoid the elastic deformation of the biological tissues. To evaluate the long-term adhesion stability in specific conditions, *i.e.* acidic condition (SGF, pH 2.0), the adhered joints were soaked in the buffer solutions for a designated period before lap-shear and 180° peeling tests.

Burst pressure quantification.

Burst pressure test was performed using a home-designed setup. Briefly, a disc-shaped porcine stomach tissues with a thickness of 1 mm and a diameter of 4 cm was fixed to the setup, and a hole with a diameter of 5 mm was created with a puncher. The ATGels samples with a diameter of 10 mm and a thickness of 200 μm were used to seal the hole, following the above-mentioned protocol. An EFD dispenser was used to control the airflow, which was gradually increased for exerting an increasing pressure on the sealed hole. The burst pressure was taken as the pressure when failure of the sealed wound occurred. Commercially-available bioadhesives, Vedbond^{TM} and Fibrin glue^{TM}, were also measured for comparison. All measurements were repeated for five times, and the data were presented as mean ± S.D. (n = 5).

Ex vivo sealing of the gastric perforation.

To demonstrate the robust and stable sutureless sealing of gastric perforation by the ATGels bioadhesive under gastric environment, porcine stomaches from local butcher's shop were used. An incision with a length of 5 cm was created with a scalpel, immediately prior to sealing with an ATGels sample (length of 5 cm, width of 3 mm and thickness of 500 μm). Afterwards, the sealed stomach was immersed into PBS buffer, and the stomach cavity was filled with SGF (pH 2.0, red food dye was used for better visual effect) to simulate the gastric environment in the body. Images of the sealed incision in the presence of SGF were taken to monitor the stability of the adhesion. Gastric incision sealed with PAA-NHS bulk hydrogels (ContGels) was also tested as a control.

Animal Experiments.

All the animal handling procedures were carried out in compliance with the standard guidelines approved by the Southern University of Science and Technology (SUSTech) Ethics Committee, and all animal surgeries were approved by the Committee on Animal Care at SUSTech (Protocol No. SUSTech-SL202101010). Male Sprague Dawley (SD) rats (200-300 g, Charles River *Co. Ltd.*) were used for this study.

In vivo gastric perforation repairing.

The SD rats were deprived of food for 12 h and water for 4 h prior to the surgery to minimize bowel contents in the stomach. The SD rats were anesthetized with isoflurane (1-2 *vol.%* isoflurane in oxygen) throughout the surgery. In order to avoid contamination of the abdominal cavity, the stomach was isolated by making an incision at the abdomen with a scalpel, rinsed with PBS solution and packed on a sterile surgical drape before establishing the gastric perforation model. The gastric perforation was made by creating a 5-mm hole at the bottom side of the stomach, and a sterile gauze was immediately used for hemostasis treatment. Our ATGels dry films (8 mm (*L*) × 6 mm (*W*) × 200 μm (*t*)) were utilized to seal the perforation by gentle pressing for 10 s (*i.e.* 1 kPa), leading to a robust sealing of the stomach (n = 15). (Note: the other side of the ATGels was treated with tiny amount of sterilized BSA solution (1 *wt.%*) to avoid postoperative adhesion during the gastric perforation healing.) The repaired gastric tissues were collected at a designated intervals (*i.e.* 7, 14 and 28 days), fixed with 4 *vol.%* paraformaldehyde/PBS solution, and then embedded in paraffin for further histological and immunohistochemical analyses. Meanwhile, gastric perforation sealed with sutures (7-0 PLGA suture, Gold ring enterprise group, Shanghai, China) was also conducted and compared as controls.

Histological analysis and immunohistochemistry.

HE and Masson staining were performed on the repaired rat gastric tissue. Briefly, the fixed tissue samples were first dehydrated in sequence using ethanol and embedded in paraf-

fin. Afterwards, the samples were cut with a Leica RM2016 Cryostat (Leica, Germany) into sections (thickness: 4 μm), followed by further hematoxylin and eosin or masson staining.

For immunohistochemical and immunofluorescence staining, the rat repaired gastric tissues were cut into sections with a thickness of 4 μm and de-paraffinized using xylene. The sections were soaked into ethanol for 10 min and then rehydrated with deionized water. Citric acid buffer (pH 6.0) was then used for antigen retrieval, prior to 25-min incubation in H_2O_2 solution (3 *wt.%*) at room temperature. After blocking the nonspecific binding sites with 3 *wt.%* BSA/PBS solution at room temperature for 30 min, the tissue samples were then treated with primary antibody (CD68 1:200, α-SMA 1:200, CD31 1:100, or PCNA 1:1000) for 4 h at 37 °C. The tissue sections were rinsed with PBS buffer and then incubated with secondary antibody (Goat anti-rabbit IgG (H+L), 1:1000) for another 60 min, followed by further staining with DAB (3, 3-diaminobenzidine, Servicebio, Wuhan, China) for peroxidase. Meanwhile, the sections were incubated with either hematoxylin for 5 min or DAPI for 10 min to stain the cell nucleus. Immunohistochemical staining and immunofluorescent images were observed using an upright microscope (Leica DM 2700M) and a laser confocal scanning microscope (CLSM, Lecia SP8), respectively. For further quantitative analysis, the percentage of the expressed antibody was analyzed with ImageJ from over 100 data points.

Statistical analysis.

All the data were processed with Origin 8.0 and presented as the mean $\pm$ S.D. One-way analysis of variance (One-way ANOVA) was used to determine the significance level between multiple groups, and the significance level was considered as $^{*}p < 0.05$, $^{**}p < 0.01$, $^{***}p < 0.001$.

Acknowledgements

J.L. acknowledges the research startup grant from Shenzhen municipal government (Y01336223) and the research startup grant from SUSTech (Y01336123)), and the financial support by MechERE Centers at MIT and SUSTech (Y01346002). This work was also supported in part by the Science, Technology and Innovation Commission of Shenzhen Municipality (ZDSYS20200811143601004), Basic and Applied Basic Research Foundation of Guangdong Province (2020A1515110288) and the Basic Research Program of Shenzhen (JCYJ20210324105211032). The authors also would like to acknowledge the technical support from SUSTech Core Research Facilities, and also thank Prof. Fuzeng Ren for his support in cell experiments.

Additional information.

Supplementary information is available in the online version of the paper. Reprints and permissions information is available online.

References

[1] R. Sitarz, M. Skierucha, J. Mielko, G. J. A. Offerhaus, R. Maciejewski, W. P. Polkowski, *Cancer Manag. Res.* **2018**, *10*, 239–248.

[2] M. A. Revell, M. A. Pugh, M. McGhee, *Crit. Care Nurs. Clin. North Am.* **2017**, *30*, 157–166.

[3] C Bloechle, A Emmermann, T Strate, U. Scheurlen, C Schneider, E Achilles, M Wolf, D Mack, C Zornig, C. Broelsch, *Surg. Endosc.* **1998**, *12*, 212–218.

[4] P. J. Bouten, M. Zonjee, J. Bender, S. T. Yauw, H. van Goor, J. C. van Hest, R. Hoogenboom, *Prog. Polym. Sci.* **2014**, *39*, 1375–1405.

[5] S. Barnes, M. Spencer, D. Graham, H. B. Johnson, *Am. J. Infect. Control* **2014**, *42*, 525–529.

[6] T. B. Reece, T. S. Maxey, I. L. Kron, *Am. J. Surg.* **2001**, *182*, 40–44.

[7] Z. A. Murrell, M. J. Stamos, *Clin. Colon Rectal. Surg.* **2006**, *19*, 213–216.

[8] A. Miyamoto, S. Lee, N. F. Cooray, S. Lee, M. Mori, N. Matsuhisa, H. Jin, L. Yoda, T. Yokota, A. Itoh, M. Sekino, H. Kawasaki, T. Ebihara, M. Amagai, T. Someya, *Nat. Nanotech.* **2017**, *12*, 907–913.

[9] C. Ghobril, M. W. Grinstaff, *Chem. Soc. Rev.* **2015**, *44*, 1820–1835.

[10] G. G. Giobbe, C. Crowley, C. Luni, S. Campinoti, M. Khedr, K. Kretzschmar, M. M. De Santis, E. Zambaiti, F. Michielin, L. Meran, Q. Hu, G. van Son, L. Urbani, A. Manfredi, M. Giomo, S. Eaton, D. Cacchiarelli, V. S. W. Li, H. Clevers, P. Bonfanti, N. Elvassore, P. De Coppi, *Nat. Commun.* **2019**, *10*, 5658.

[11] G. M. Taboada, K. Yang, M. J. Pereira, S. S. Liu, Y. Hu, J. M. Karp, N. Artzi, Y. Lee, *Nat. Rev. Mater.* **2020**, 310–329.

[12] W. Zhu, Y. J. Chuah, D.-A. Wang, *Acta Biomater.* **2018**, *74*, 1–16.

[13] X. Liu, J. Liu, S. Lin, X. Zhao, *Mater. Today* **2020**, *36*, 102–124.

[14] X. Peng, X. Xia, X. Xu, X. Yang, B. Yang, P. Zhao, W. Yuan, P. W. Y. Chiu, L. Bian, *Sci. Adv.* **2021**, *7*, eabe8739.

[15] D. Gan, W. Xing, L. Jiang, J. Fang, C. Zhao, F. Ren, L. Fang, K. Wang, X. Lu, *Nat. Commun.* **2019**, *10*, 1487.

[16] Y. Wang, L. Shang, G. Chen, L. Sun, X. Zhang, Y. Zhao, *Sci. Adv.* **2020**, *6*, eaax8258.

[17] H. Yuk, C. E. Varela, C. S. Nabzdyk, X. Mao, R. F. Padera, E. T. Roche, X. Zhao, *Nature* **2019**, *575*, 169–174.

[18] Y. Xue, J. Zhang, X. Chen, J. Zhang, G. Chen, K. Zhang, J. Lin, C. Guo, J. Liu, *Adv. Funct. Mater.* **2021**, *31*, 2106446.

[19] K. Zhang, X. Chen, Y. Xue, J. Lin, X. Liang, J. Zhang, J. Zhang, G. Chen, C. Cai, J. Liu, *Adv. Funct. Mater.* **2022**, *32*, 2111465.

[20] E. S. Sani, A. Kheirkhah, D. Rana, Z. Sun, W. Foulsham, A. Sheikhi, A. Khademhosseini, R. Dana, N. Annabi, *Sci. Adv.* **2019**, *5*, eaav1281.

[21] Y. Hong, F. Zhou, Y. Hua, X. Zhang, C. Ni, D. Pan, Y. Zhang, D. Jiang, L. Yang, Q. Lin, Y. Zou, D. Yu, D. E. Arnot, X. Zou, L. Zhu, S. Zhang, H. Ouyang, *Nat. Commun.* **2019**, *10*, 2060.

[22] J. Li, A. Celiz, J Yang, Q Yang, I Wamala, W Whyte, B. Seo, N. Vasilyev, J. Vlassak, Z Suo, D. J. Mooney, *Science* **2017**, *357*, 378–381.

[23] Y. Liu, J. Liu, S. Chen, T. Lei, Y. Kim, S. Niu, H. Wang, X. Wang, A. M. Foudeh, J. B.-H. Tok, Z. Bao, *Nat. Biomed. Eng.* **2019**, *3*, 58–68.

[24] J. Liu, C. S. Y. Tan, O. A. Scherman, *Angew. Chem. Int. Ed.* **2018**, *130*, 8992–8996.

[25] J. Liu, O. A. Scherman, *Adv. Funct. Mater.* **2018**, *28*, 1800848.

[26] C. Cui, T. Wu, X. Chen, Y. Liu, Y. Li, Z. Xu, C. Fan, W. Liu, *Adv. Funct. Mater.* **2020**, *30*, 2005689.

[27] X. Xu, X. Xia, K. Zhang, A. Rai, Z. Li, P. Zhao, K. Wei, L. Zou, B. Yang, W.-K. Wong, P. W. Chiu, L. Bian, *Sci. Transl. Med.* **2020**, *12*, 558.

[28] J. He, Z. Zhang, Y. Yang, F. Ren, J. Li, S. Zhu, F. Ma, R. Wu, Y. Lv, G. He, B. Guo, D. Chu, *Nano-Micro Lett.* **2021**, *13*, 1–17.

[29] B. Liu, Y. Wang, Y. Miao, X. Zhang, Z. Fan, G. Singh, X. Zhang, K. Xu, B. Li, Z. Hu, M. Xing, *Biomaterials* **2018**, *171*, 83–96.

[30] T. V. Berne, A. J. Donovan, *Arch. Surg.* **1989**, *124*, 830–832.

[31] K. Sumiyama, C. J. Gostout, E. Rajan, T. A. Bakken, J. L. Deters, M. A. Knipschield, *Gastrointest. Endosc.* **2007**, *65*, 134–139.

[32] H. S. Kim, J. H. Lee, M. G. Kim, *Surg. Endosc.* **2021**, *35*, 4206–4213.

[33] M. Ozmen, B Zulfikaroglu, C Kece, A. Aslar, N Ozalp, M Koc, *J. Int. Med. Res.* **2002**, *30*, 180–184.

[34] X. Liu, C. Steiger, S. Lin, G. A. Parada, J. Liu, H. F. Chan, H. Yuk, N. V. Phan, J. Collins, S. Tamang, G. Traverso, X. Zhao, *Nat. Commun.* **2019**, *10*, 493.

[35] J. Liu, S. Lin, X. Liu, Z. Qin, Y. Yang, J. Zang, X. Zhao, *Nat. Commun.* **2020**, *11*, 1071.

[36] M. F. Refojo, *J. Polym. Sci. Polym. Chem.* **1967**, *5*, 3103–3113.

[37] F. J. Holly, M. F. Refojo, *J. Biomed. Mater. Res.* **1975**, *9*, 315–326.

[38] S. J. Wu, H. Yuk, J. Wu, C. S. Nabzdyk, X. Zhao, *Adv. Mater.* **2021**, *33*, 2007667.

[39] N. Lang, M. J. Pereira, Y. Lee, I. Friehs, N. V. Vasilyev, E. N. Feins, K. Ablasser, E. D. OCearbhaill, C. Xu, A. Fabozzo, R. Padera, S. Wasserman, F. Freudenthal, L. S. Ferreira, R. Langer, J. M. Karp, P. J. del Nido, *Sci. Transl. Med.* **2014**, *6*, 218ra6–218ra6.

[40] S Yarrow, J Hare, K. Robinson, *Anaesthesia* **2003**, *58*, 1019–1022.

[41] Y. Bu, L. Zhang, G. Sun, F. Sun, J. Liu, F. Yang, P. Tang, D. Wu, *Adv. Mater.* **2019**, *31*, 1901580.

[42] A. Nishiguchi, F. Sasaki, H. Maeda, M. Kabayama, A. Ido, T. Taguchi, *Small* **2019**, *15*, 1901566.

[43] J. L. Wallace, *Am. J. Med.* **2001**, *110*, S19–S23.

Entry for the Table of Contents (Please choose one layout only)

Layout 1:

Catch Phrase:

Author(s), Corresponding Author(s) . . . . . Page Page*

Title Text

((The TOC Graphic should not exceed the size of this area))

Text for Table of Contents, max. 450 characters.

Layout 2:

Hydrogel Bioadhesives with Extreme Acid-Tolerance

*Xingmei Chen,[a] Jun Zhang,[a] Guangda Chen,[a] Yu Xue,[a] Jiajun Zhang,[a] Xiangyu Liang,[a] Iek Man Lei,[a] Jingsen Lin,[a] Ben Bin Xu[b] and Ji Liu[a,c,d]**

Hydrogel Bioadhesives with Extreme Acid-Tolerance for Gastric Perforation Repairing

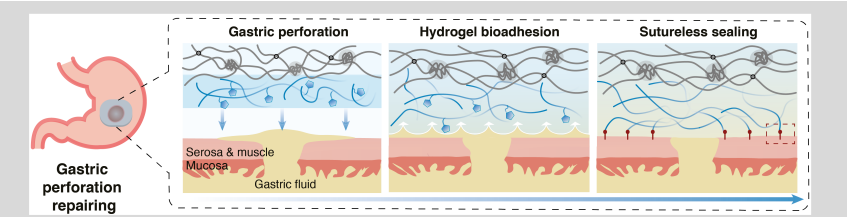

Gastric Perforation Repairing with Hydrogel Bioadhesives: A kind of synthetic hydrogel bioadhesives, featuring superior superior acid-tolerance, instant and robust bioadhesion, enable accelerated gastric perforation repairing.